

# Reaction of electron-deficient 6-methoxyquinolate-substituted cluster $[\text{Os}_3(\text{CO})_9\{\mu_3\text{-}\eta^1, \kappa^1\text{-C}_9\text{H}_5\text{N}(6\text{-OMe})\}(\mu\text{-H})]$ with $\text{PPh}_3$ : Thermally induced ligand isomerization, decarbonylation and orthometallation

Shahin A. Begum <sup>a</sup>, Md. Arshad H. Chowdhury <sup>a</sup>, Shishir Ghosh <sup>a</sup>, Derek A. Tocher <sup>b</sup>, Edward Rosenberg <sup>c</sup>, Kenneth I. Hardcastle <sup>d</sup>, Shariff E. Kabir <sup>a,\*</sup>

<sup>a</sup> *Department of Chemistry, Jahangirnagar University, Savar, Dhaka-1342, Bangladesh*

<sup>b</sup> *Department of Chemistry, University College London, 20 Gordon Street, London WC1H 0AJ, UK*

<sup>c</sup> *Department of Chemistry, University of Montana, Missoula, Montana 58912, USA*

<sup>d</sup> *Department of Chemistry, Emory University, Atlanta, Georgia 30322, USA*

\* Corresponding author.

E-mail address: skabir\_ju@yahoo.com (S.E. Kabir).

Tel.: +880 27791099; fax: +880 27791052.

## ABSTRACT

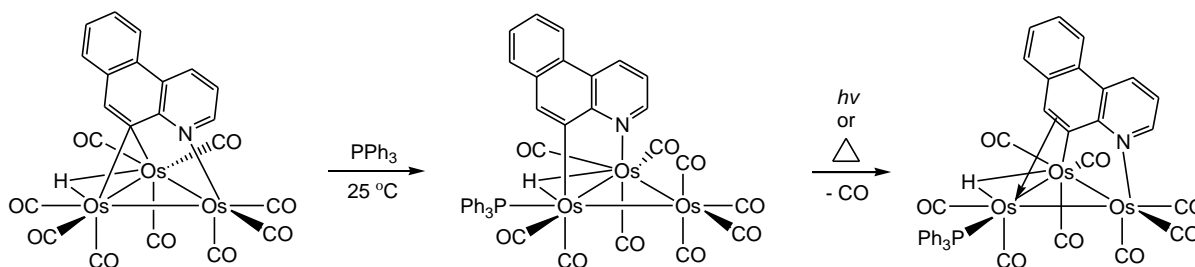
The reaction of the electron-deficient 6-methoxyquinolate-substituted triosmium cluster  $[\text{Os}_3(\text{CO})_9\{\mu_3\text{-}\eta^1, \kappa^1\text{-C}_9\text{H}_5\text{N}(6\text{-OMe})\}(\mu\text{-H})]$  (**1**) with  $\text{PPh}_3$  proceeds readily at room temperature to afford the electron-precise adduct  $[\text{Os}_3(\text{CO})_9(\text{PPh}_3)\{\mu\text{-}\eta^1, \kappa^1\text{-C}_9\text{H}_5\text{N}(6\text{-OMe})\}(\mu\text{-H})]$  (**2**), in which the  $\text{PPh}_3$  ligand is bound to the osmium that serves as the coordination site for the hydride and the metallated-carbon atom of the benzoheterocycle. This reaction also leads to a change in the hapticity of the 6-methoxyquinolate ligand from  $\mu_3\text{-}\eta^1, \kappa^1$  to  $\mu\text{-}\eta^1, \kappa^1$  as confirmed by X-ray crystallography. Thermolysis of **2** in boiling toluene furnishes five new triosmium clusters (**3-7**) as a result of ligand isomerization, decarbonylation and orthometallation of the ancillary  $\text{PPh}_3$  ligand. Clusters **3** and **4** are isomers of **2** and the location of the metal-bound hydride and  $\text{PPh}_3$  with respect to 6-methoxyquinolate moiety is the only difference between these isomers. Control experiments show that **5** is a decarbonylation product of **4** which converts in to **6** as a result of further decarbonylation with concomitant orthometallation of one of the phenyl rings of the coordinated  $\text{PPh}_3$  ligand, whilst **7** is formed from **6** through replacement of an equatorial

carbonyl of the nitrogen-bound osmium by PPh<sub>3</sub> ligand. All the new clusters have been characterized by a combination of analytical and spectroscopic methods as well as by X-ray crystallography in the case of **2**, **3**, **6** and **7**.

*Keywords:* Triosmium clusters; 6-Methoxyquinoline; Triphenylphosphine; Isomerization; Decarbonylation; Orthometallation

## 1. Introduction

The chemistry of electron-deficient triosmium clusters of the general formula [Os<sub>3</sub>(CO)<sub>9</sub>(μ<sub>3</sub>-η<sup>1</sup>,κ<sup>1</sup>-L)(μ-H)] (L-H = benzoheterocycle containing a pyridinyl nitrogen) have received considerable attention over the past two decades. These clusters have been used to functionalize heterocyclic substrates *via* cluster-promoted ligand activation, resulting in the synthesis of many potentially useful compounds that are not easy to obtain *via* conventional organic methods [1-26]. They also readily react with two electron donor ligands such as tertiary phosphines at ambient temperature to give electron-precise adducts. Studies also showed that the nature of the heterocyclic ligands somehow influences the reactivity of the resultant phosphine adducts. For example, photolysis or thermolysis of these phosphine adducts usually leads to nonspecific decomposition or phosphine ligand dissociation to give the phosphine-free nona- and deca-carbonyl clusters [Os<sub>3</sub>(CO)<sub>9</sub>(μ<sub>3</sub>-η<sup>1</sup>,κ<sup>1</sup>-L)(μ-H)] and [Os<sub>3</sub>(CO)<sub>10</sub>(μ-η<sup>1</sup>,κ<sup>1</sup>-L)(μ-H)] [3,8]. However, an electron-precise σ-π vinyl complex was formed *via* carbonyl dissociation upon photolysis or thermolysis in the case of metallated 5,6-benzoquinolate cluster as shown in Scheme 1 [8].



**Scheme 1.** Reactivity of [Os<sub>3</sub>(CO)<sub>9</sub>(μ<sub>3</sub>-η<sup>1</sup>,κ<sup>1</sup>-C<sub>13</sub>H<sub>8</sub>N)(μ-H)] towards PPh<sub>3</sub> [8].

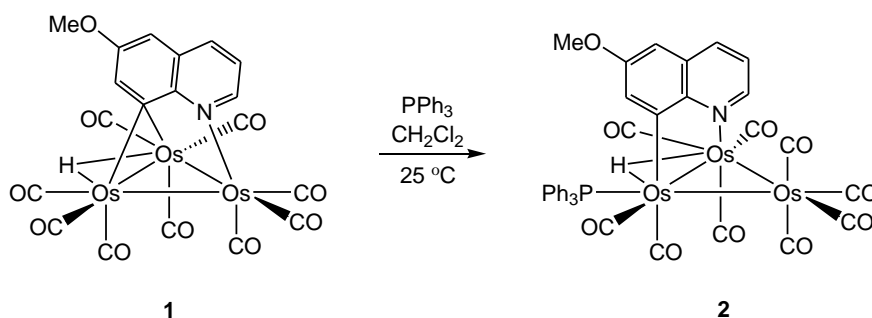
As part of our studies on the reactivity of electron-deficient  $[\text{Os}_3(\text{CO})_9(\mu_3\text{-}\eta^1, \kappa^1\text{-L})(\mu\text{-H})]$  with two electron donor ligands, we recently reported the reactions of benzothiazolate triosmium clusters  $[\text{Os}_3(\text{CO})_9(\mu_3\text{-}\eta^1, \kappa^1\text{-C}_7\text{H}_3\text{NSR})(\mu\text{-H})]$  ( $\text{R} = \text{H}, \text{Me}$ ) with  $\text{PPh}_3$  that led to the isolation of electron-precise adducts  $[\text{Os}_3(\text{CO})_9(\text{PPh}_3)(\mu, \eta^2\text{-C}_7\text{H}_3\text{NSR})(\mu\text{-H})]$  in which  $\text{PPh}_3$  ligand occupies an equatorial site at the carbon bound osmium. Thermolysis of these adducts afforded a number of products resulting from isomerization, decarbonylation and orthometallation of the ancillary  $\text{PPh}_3$  ligand [27]. As a continuation of our previous studies, we have now investigated the reactivity 6-methoxyquinolate triosmium cluster  $[\text{Os}_3(\text{CO})_9\{\mu_3\text{-}\eta^1, \kappa^1\text{-C}_9\text{H}_5\text{N}(6\text{-OMe})\}(\mu\text{-H})]$  (**1**) with  $\text{PPh}_3$ . The aim of this study was to understand the influence of benzoheterocyclic ligands on the reactivity of  $[\text{Os}_3(\text{CO})_9(\mu_3\text{-}\eta^1, \kappa^1\text{-L})(\mu\text{-H})]$  towards  $\text{PPh}_3$  by comparing the reactivity of **1** towards  $\text{PPh}_3$  with that of other electron-deficient triosmium cluster containing different benzoheterocyclic ligands e.g. quinolate [5], 5,6-benzoquinolate [8], benzothiazolate [27] and 2-methylbenzothiazolate [27].

## 2. Results and discussion

### 2.1. Formation of $\text{PPh}_3$ adduct of $[\text{Os}_3(\text{CO})_9\{\mu_3\text{-}\eta^1, \kappa^1\text{-C}_9\text{H}_5\text{N}(6\text{-OMe})\}(\mu\text{-H})]$ (**1**)

Reaction of electron-deficient **1** with  $\text{PPh}_3$  proceeded smoothly at room temperature to furnish electron-precise  $[\text{Os}_3(\text{CO})_9(\text{PPh}_3)\{\mu\text{-}\eta^1, \kappa^1\text{-C}_9\text{H}_5\text{N}(6\text{-OMe})\}(\mu\text{-H})]$  (**2**) in almost quantitative yield (Scheme 2). Compound **2** was isolated by chromatography over silica gel, and was characterized by X-ray crystallography and spectroscopic techniques. Fig. 1 shows the solid-state molecular structure of **2** with the caption containing selected metric parameters. The cluster core consists of a metallic triangle of osmium atoms with three approximately equal Os–Os bonds [Os(1)–Os(2) 2.9009(2), Os(1)–Os(3) 2.9046(2), Os(2)–Os(3) 2.8928(2) Å] which is coordinated by nine carbonyls, a 6-methoxyquinolate, a  $\text{PPh}_3$  and a hydride ligand. The 6-methoxyquinolate moiety functions as a 3e donor and tethers the Os(1)–Os(2) bond in an edge-bridging fashion. The hydride ligand which was located crystallographically also spans the same osmium-osmium edge. The  $\text{PPh}_3$  ligand occupies an equatorial site at the Os(1) center *cis* to the hydride that also serves as the coordination site for the metallated carbon atom, C(10), on the 6-methoxyquinolate ligand. The gross structural features of **2** are virtually identical to those reported for the related triosmium

clusters  $[\text{Os}_3(\text{CO})_9(\text{PPh}_3)(\mu\text{-}\eta^1, \kappa^1\text{-C}_7\text{H}_3\text{NSR})(\mu\text{-H})]$  ( $\text{R} = \text{H}, \text{Me}$ ) [27],  $[\text{Os}_3(\text{CO})_9(\text{PPh}_3)(\mu\text{-}\eta^1, \kappa^1\text{-C}_{13}\text{H}_8\text{N})(\mu\text{-H})]$  [8] and  $[\text{Os}_3(\text{CO})_9\{\text{P}(\text{OEt})_3\}(\mu\text{-}\eta^1, \kappa^1\text{-C}_9\text{H}_5\text{NMe})(\mu\text{-H})]$  [5].

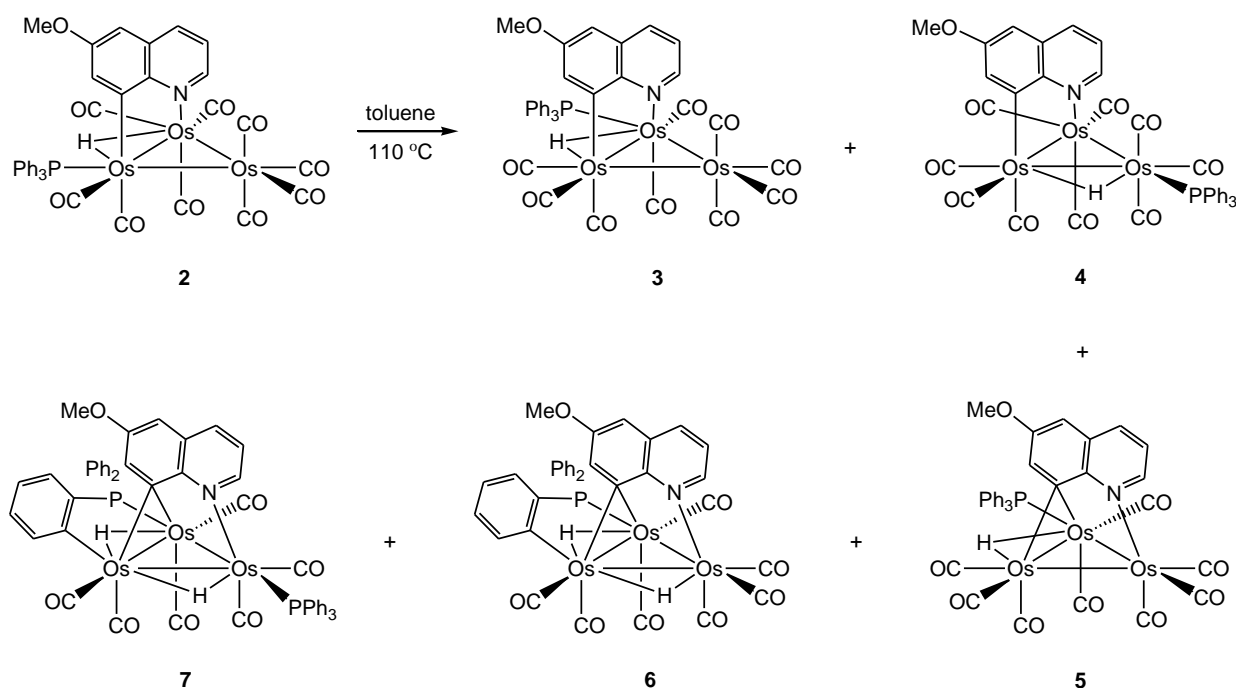


**Scheme 2.** Reaction of  $[\text{Os}_3(\text{CO})_9\{\mu_3\text{-}\eta^1, \kappa^1\text{-C}_9\text{H}_5\text{N}(6\text{-OMe})\}(\mu\text{-H})]$  (**1**) with  $\text{PPh}_3$ .

The spectroscopic data of **2** indicate that the solid-state structure persists in solution. The  $^{31}\text{P}\{^1\text{H}\}$  NMR spectrum exhibits a singlet at  $\delta$  12.6 due to the  $\text{PPh}_3$  ligand, whilst the  $^1\text{H}$  NMR spectrum display a high-field doublet  $\delta$   $-11.76$  ( $J$  15.6 Hz) for the bridging hydride, together with expected number of resonances in the aromatic region for the phenyl and 6-methoxyquinoline ring protons. The  $^1\text{H}$  NMR spectrum of **2** also exhibits a 3H singlet at  $\delta$  3.58 for the 6-OMe group on the quinolate ring.

## 2.2. Thermolysis of $[\text{Os}_3(\text{CO})_9(\text{PPh}_3)\{\mu_3\text{-}\eta^1, \kappa^1\text{-C}_9\text{H}_5\text{N}(6\text{-OMe})\}(\mu\text{-H})]$ (**2**)

Heating a toluene solution of **2** at 110 °C led to the isolation of five new clusters  $[\text{Os}_3(\text{CO})_9(\text{PPh}_3)\{\mu_3\text{-}\eta^1, \kappa^1\text{-C}_9\text{H}_5\text{N}(6\text{-OMe})\}(\mu\text{-H})]$  (**3,4**),  $[\text{Os}_3(\text{CO})_8(\text{PPh}_3)\{\mu_3\text{-}\eta^1, \kappa^1\text{-C}_9\text{H}_5\text{N}(6\text{-OMe})\}(\mu\text{-H})]$  (**5**),  $[\text{Os}_3(\text{CO})_7\{\mu_3\text{-}\eta^1, \kappa^1\text{-PPh}_2(\text{C}_6\text{H}_4)\}\{\mu_3\text{-}\eta^1, \kappa^1\text{-C}_9\text{H}_5\text{N}(\text{OMe})\}(\mu\text{-H})_2]$  (**6**) and  $[\text{Os}_3(\text{CO})_6(\text{PPh}_3)\{\mu_3\text{-}\eta^1, \kappa^1\text{-PPh}_2(\text{C}_6\text{H}_4)\}\{\mu_3\text{-}\eta^1, \kappa^1\text{-C}_9\text{H}_5\text{N}(\text{OMe})\}(\mu\text{-H})_2]$  (**7**), after usual chromatographic separation and work up (Scheme 3). Clusters **3** and **4** are isomers of **2** that results from a complex rearrangement of the ligands about the cluster polyhedron. Cluster **5** was isolated in small yield as a result of formal decarbonylation of **2**. In separate experiments, we also showed that cluster **5** decarbonylated further to form **6** via orthometallation of one of the aryl rings of the coordinated phosphine which reacted further with a molecule of  $\text{PPh}_3$  to furnish **7**. All of these thermolysis products have been characterized by analytical and spectroscopic methods together with single crystal X-ray diffraction analyses for **3**, **6** and **7**.



**Scheme 3.** Thermolysis of  $[\text{Os}_3(\text{CO})_9(\text{PPh}_3)\{\mu\text{-}\eta^1, \kappa^1\text{-C}_9\text{H}_5\text{N}(6\text{-OMe})\}(\mu\text{-H})]$  (**2**).

### 2.3. Cluster isomers **3** and **4**

The IR spectrum recorded for **3** are nearly identical with that of **2** which indicates that these clusters have relatively similar distribution of carbonyl ligands about the  $\text{Os}_3$  polyhedron. Cluster **3** displays a high-field hydride doublet at  $\delta -12.13$  ( $J_{\text{P-H}}$  16.8 Hz) in its  $^1\text{H}$  NMR spectrum together with resonances expected for phenyl, quinoline and methoxy protons, whilst it exhibits a single isomer in the  $^{31}\text{P}\{^1\text{H}\}$  NMR spectrum. We also carried out single crystal X-ray diffraction analysis for **3**, the results of which are shown in Fig. 2. The molecule consists of a triangular array of osmium atoms where the osmium-osmium bond distances range from 2.8936(2) [Os(1)–Os(3)] to 2.9131(2) Å [Os(2)–Os(3)], a pattern that is also reflected in the osmium-osmium bond distances displayed by **2**. Present in the metal coordination sphere are nine terminal carbonyl ligands, four bonded to Os(3), three to Os(2) and two to Os(1), one edge-bridging 6-methoxyquinolinate ligand, one edge bridging hydride, and a  $\text{PPh}_3$  ligand. The hydride ligand was crystallographically located across the Os(1)–Os(2) edge which is also bridged by the 6-methoxyquinolinate ligand. The  $\text{PPh}_3$  ligand occupies an equatorial site on Os(1) that is directly bound to the metallated N(1) atom on the 6-methoxyquinoline ligand. The Os–P distance [2.3690(10) Å] is identical to that found in **2**.

The gross structural features of **3** are very similar to those reported for the related benzothiazolate triosmium cluster  $[\text{Os}_3(\text{CO})_9(\text{PPh}_3)(\mu\text{-}\eta^1, \kappa^1\text{-C}_7\text{H}_3\text{NSMe})(\mu\text{-H})]$  [27], in which the  $\text{PPh}_3$  ligand also occupies an equatorial site at the nitrogen bound osmium atom.

We were unable to obtain single crystals of **4** suitable for X-ray diffraction analysis, so its structure was formulated using the data obtained from analytical and spectroscopic studies. The solution spectroscopic data recorded for **4** also indicate a close structural similarity with **2** and **3**. Cluster **4** can be straightforwardly characterized by comparing its IR spectrum with that of  $[\text{Os}_3(\text{CO})_9(\text{PPh}_3)(\mu\text{-}\eta^1, \kappa^1\text{-C}_7\text{H}_3\text{NSMe})(\mu\text{-H})]$  [27] which was obtained from the thermolysis of  $[\text{Os}_3(\text{CO})_9(\text{PPh}_3)(\mu\text{-}\eta^1, \kappa^1\text{-C}_7\text{H}_3\text{NSMe})(\mu\text{-H})]$ . This benzothiazolate triosmium cluster was characterized by single crystal X-ray diffraction analysis in which the hydride and heterocyclic ligand span different osmium-osmium edges with the  $\text{PPh}_3$  ligand occupying an equatorial site at the rear osmium atom [27]. The  $^1\text{H}$  NMR spectrum of **4** shows a high-field doublet at  $\delta -15.58$  ( $J_{\text{P-H}}$  14.0 Hz) for the hydride and a 3H singlet at  $\delta 3.96$  due to the methoxy protons. The spectrum also exhibits five well-separated multiplets attributed to the quinoline ring protons; three doublets of doublets at  $\delta 9.57$  (J 5.6, 1.2 Hz), 7.89 (J 8.0, 1.2 Hz,) and 7.06 (J 8.0, 5.6 Hz) and two doublets at  $\delta 8.31$  (J 2.8 Hz) and 6.63 (J 2.8 Hz), while the phenyl ring protons appeared as a 15H multiplet centered at  $\delta 7.35$ . The  $^{31}\text{P}\{^1\text{H}\}$  NMR displays single resonance at  $\delta -3.2$  for the  $\text{PPh}_3$  ligand.

#### 2.4. Decarbonylation products 5-7

Repeated attempts to grow single crystals of **5** were unsuccessful, so it has been characterized by analytical and spectroscopic data. The IR spectrum of **5** is virtually identical to that of the structurally characterized benzothiazolate cluster  $\text{Os}_3(\text{CO})_8(\text{PPh}_3)\{\mu_3\text{-}\eta^1, \kappa^1\text{-C}_7\text{H}_3\text{NSMe})(\mu\text{-H})$  [27], indicating that the two clusters are structurally similar. The combustion data are consistent with the proposed structure. In addition to the phenyl proton resonances appeared as a multiplet centered at  $\delta 7.38$  (m, 15H), the  $^1\text{H}$  NMR spectrum of **5** also exhibits five well-separated resonances for the quinoline ring protons; three doublets of doublets at  $\delta 9.48$  (J 5.2, 1.6, Hz), 7.91 (J 7.6, 1.6, Hz) and 7.12 (J 7.6, 5.2, Hz) and two doublets at  $\delta 8.35$  (J 2.8 Hz) and 6.58 (J 2.8 Hz). The hydride resonance is observed as a doublet at  $\delta -10.25$  ( $J_{\text{P-H}}$  7.6 Hz) while the 3H singlet at  $\delta 3.94$  is assigned to the methoxy protons. The  $^{31}\text{P}\{^1\text{H}\}$  NMR shows single resonance at  $\delta 22.2$  for the  $\text{PPh}_3$  ligand as expected. The hydride and the  $^{31}\text{P}$  chemical shifts of **5** are also very similar to those reported for  $[\text{Os}_3(\text{CO})_8(\text{PPh}_3)\{\mu_3\text{-}\eta^1, \kappa^1\text{-}$

$C_7H_3NSMe)(\mu-H)]$  (hydride:  $\delta -10.21$ ,  $J_{P-H}$  8.8 Hz;  $^{31}P$ :  $\delta 22.5$ ) [27], in which the benzothiazolate ligand caps one face of the cluster while the hydride spans an osmium-osmium edge with the  $PPh_3$  ligand occupying an equatorial site at the carbon bound osmium atom.

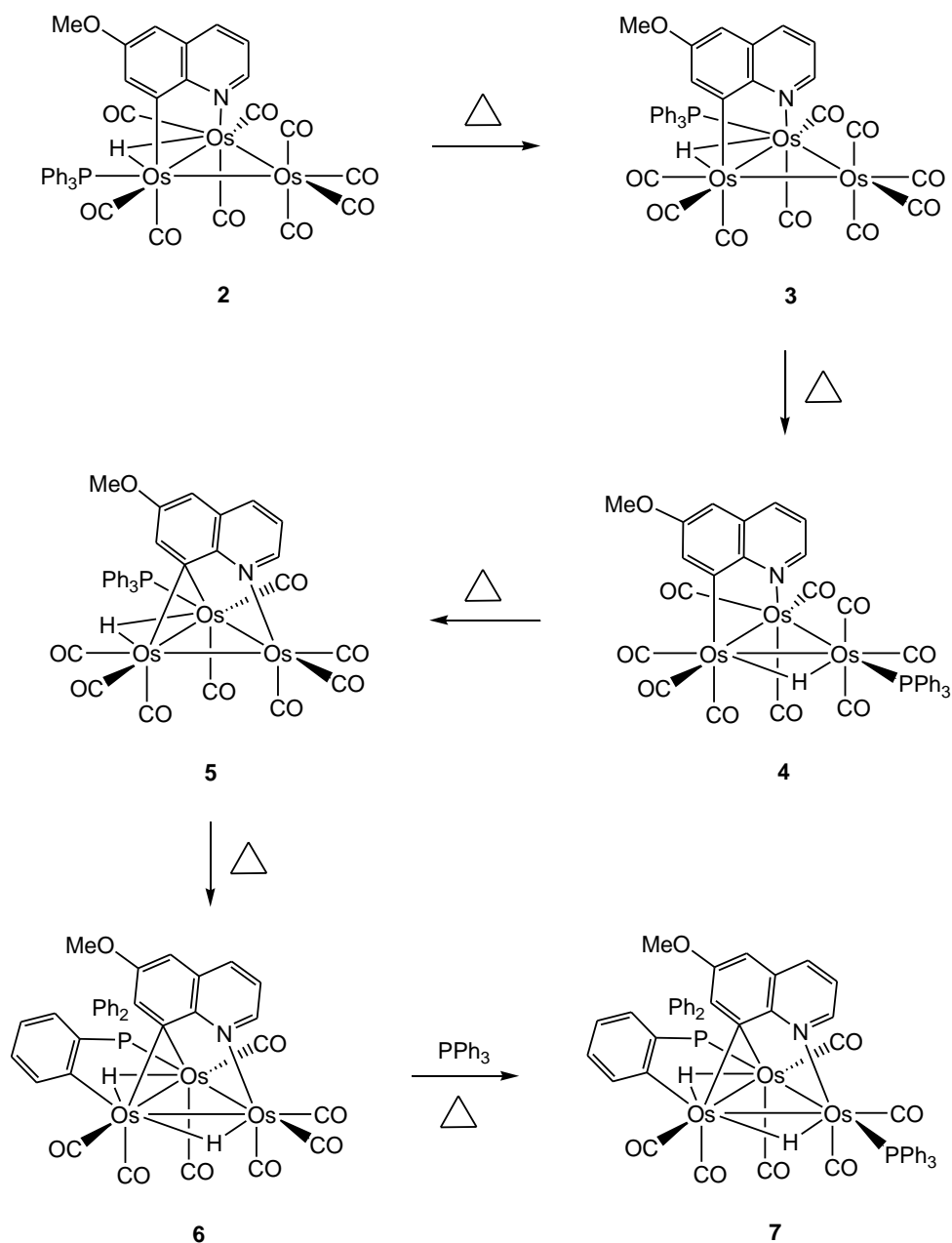
As mentioned earlier, decarbonylation of **5** followed by concomitant orthometallation of one of the aryl rings of the coordinated phosphine afforded **6** which reacted further with  $PPh_3$  to give **7**. Both these orthometallated clusters have been characterized by analytical and spectroscopic techniques together with single crystal X-ray diffraction analysis. The solid-state molecular structure of **6** is depicted in Fig. 3 with selected bond lengths and angles listed in the figure caption. The molecule consists of an  $Os_3$  triangle with two short [ $Os(1)-Os(2)$  2.7765(5) and  $Os(1)-Os(3)$  2.7152(5) Å] and one significantly longer [ $Os(2)-Os(3)$  2.9918(5) Å] osmium-osmium distances. The  $Os(2)$  is ligated by three CO groups, while  $Os(1)$  and  $Os(3)$  are coordinated to two CO groups. The 6-methoxyquinolate ring is bound to the cluster through coordination of the nitrogen lone pair to  $Os(2)$  and by participating in a three center-two electron bond using the C(8) carbon which symmetrically spans the  $Os(1)-Os(3)$  edge [ $Os(2)-C(8)$  2.310(7),  $Os(3)-C(8)$  2.301(7) Å]. The orthometallated phosphine ligand bridges the shortest osmium-osmium edge [ $Os(1)-Os(3)$ ] through the metallated phenyl group of the  $PPh_3$  ligand. The hydride ligands were not located from the structural studies and were calculated from the structural data using the program XHYDEX which were found to bridge the shortest [ $Os(1)-Os(3)$ ] and the longest [ $Os(1)-Os(2)$ ] osmium-osmium edges. This finding is also reinforced by the  $C(13)-Os(2)-Os(1)$  angle of  $118.37(13)^\circ$  along this edge which is widened significantly as compared to the related  $C(15)-Os(2)-Os(3)$  angle of  $83.43(13)^\circ$  along the  $Os(2)-Os(3)$  edge. The overall structural features of **6** are very similar to those observed for the benzothioazolate cluster  $[Os_3(CO)_7\{\mu-\eta^1,\kappa^1-PPh_2(C_6H_4)\}(\mu_3-\eta^1,\kappa^1-C_7H_3NSMe)(\mu-H)_2]$  [27]. The spectroscopic data of **6** are fully consistent with the solid-state structure. The  $^{31}P\{^1H\}$  NMR spectrum shows single resonance at  $\delta -22.9$ , whilst the  $^1H$  NMR spectrum exhibits two high-field hydride resonances [a doublet at  $\delta -9.04$  ( $J_{P-H}$  12.4 Hz) and a singlet at  $\delta -11.43$ ] as expected and a 3H singlet at  $\delta 3.39$  for the methoxyprotons in addition to resonances observed in the aromatic region for the phenyl and quinoline ring protons.

The solid-state molecular structure of **7** is depicted in Fig. 4 with the caption containing selected bond lengths and bond angles. Akin to **6**, the cluster core contains an osmium

triangle with two short [Os(1)–Os(2) 2.7765(5), Os(1)–Os(3) 2.7152(5) Å] and one relatively long [Os(2)–Os(3) 2.9918(5) Å] osmium-osmium distances. The metallic core is coordinated by six terminal carbonyls which are evenly distributed to three osmium atoms. A triply bridging 6-methoxyquinolate ligand caps one face of the metal triangle and serves as a 3e donor as observed in **6**. The orthometallated phosphine bridges the shortest osmium-osmium edge [Os(2)–Os(3)], while the other occupies an equatorial coordination site at the nitrogen-bound osmium, Os(2). The positions of the two bridging hydrides were calculated with HYDEX which show that they bridge the Os(1)–Os(3) and Os(2)–Os(3) edges. The basic architecture of **7** is similar to that of **6** except that one of the equatorial CO on the nitrogen-bound osmium in **6** is replaced by a PPh<sub>3</sub> ligand in **7**. The solution spectroscopic data of **7** are in accord with the solid-state structure. In particular, the <sup>1</sup>H NMR shows two equal intensity hydride resonances, a doublet of doublets at δ –8.76 (J 12.0, 2.4, Hz) and a doublet at δ –11.22 (J 18.0 Hz), each integrating to one proton. The <sup>31</sup>P{<sup>1</sup>H} NMR spectrum shows two singlets at δ 13.2 and –18.2.

### 3. Conclusions

In summary, the room temperature reaction between electron-deficient **1** and PPh<sub>3</sub> affords the electron-precise adducts **2** in which the PPh<sub>3</sub> ligand occupies an equatorial site to the carbon-bound osmium atom. Upon heating **2** undergoes complex transformations to form five new clusters **3-7**. Clusters **3** and **4** are more stable isomers of **2** and resulted from the rearrangement of hydride and PPh<sub>3</sub> ligands relative to the heterocyclic ligand about the cluster polyhedron. Cluster **5** is formed *via* decarbonylation and it decarbonylates further with concomitant orthometallation of one of the aryl rings of the coordinated PPh<sub>3</sub> ligand to afford **6**. Cluster **6** reacts with PPh<sub>3</sub> to give **7** and the inter-convertibility of these products as shown in [scheme 4](#) has been checked by a series of control experiments. The present study shows that the reactivity of 6-methoxyquinolate triosmium cluster **1** towards PPh<sub>3</sub> almost parallels those observed for the benzothiazolate triosmium clusters [Os<sub>3</sub>(CO)<sub>9</sub>(PPh<sub>3</sub>)(μ,η<sup>2</sup>-C<sub>7</sub>H<sub>3</sub>NSR)(μ-H)] (R = H, Me) [27], but is quite different from those observed for its quinolate [3,5] and 5,6-benzoquinolate analogs [8]. This study also confirms that a small change in the benzoheterocycle significantly affects the reactivity of the resultant phosphine adducts of these electron-deficient clusters towards phosphines.



**Scheme 4.** Thermolysis behavior for clusters **2** through **7**.

## 4. Experimental

### 4.1. General remarks

All reactions were carried out under an inert atmosphere of nitrogen using standard Schlenk techniques unless otherwise stated. Reagent grade solvents were dried by the standard methods and were freshly distilled prior to use. Infrared spectra were recorded on Shimadzu

IR Prestige-21 spectrophotometer.  $^1\text{H}$  and  $^{31}\text{P}\{^1\text{H}\}$  NMR spectra were recorded on a Bruker Avance III HD (400 MHz) instrument. Chemical shifts were measured relative to residual protons of the deuterated solvents ( $^1\text{H}$ ) and to external 85%  $\text{H}_3\text{PO}_4$  ( $^{31}\text{P}$ ). All chemical shifts are reported in  $\delta$  units and are referenced to the residual protons of the deuterated solvents ( $^1\text{H}$ ) and to external 85%  $\text{H}_3\text{PO}_4$  ( $^{31}\text{P}$ ). The parent cluster  $[\text{Os}_3(\text{CO})_9\{\mu_3\text{-C}_9\text{H}_5\text{N}(6\text{-OMe})\}(\mu\text{-H})]$  (**1**) was prepared according to the published procedures [2] and characterized by IR and NMR spectra. Elemental analyses were performed by the Microanalytical Laboratories of the Wazed Miah Science Research Centre at Jahangirnagar University. Products were separated in the air by TLC plates coated with 0.5 mm of silica gel (HF254-type 60, E. Merck, Germany).

#### 4.2. Reaction of $[\text{Os}_3(\text{CO})_9\{\mu_3\text{-}\eta^1, \kappa^1\text{-C}_9\text{H}_5\text{N}(6\text{-OMe})\}(\mu\text{-H})]$ (**1**) with $\text{PPh}_3$

A  $\text{CH}_2\text{Cl}_2$  solution (25 mL) of **1** (100 mg, 0.102 mmol) and  $\text{PPh}_3$  (27 mg, 0.103 mmol) was stirred at room temperature for 2.5 h during which time the color of the reaction mixture changed from green to yellow. The solvent was removed under reduced pressure and the residue subjected to TLC on silica gel. Elution with hexane/ $\text{CH}_2\text{Cl}_2$  (1:1, v/v) developed a band which afforded  $[\text{Os}_3(\text{CO})_9(\text{PPh}_3)\{\mu\text{-}\eta^1, \kappa^1\text{-C}_9\text{H}_5\text{N}(6\text{-OMe})\}(\mu\text{-H})]$  (**2**) (123 mg, 97%) as yellow crystals after recrystallization from hexane/ $\text{CH}_2\text{Cl}_2$  at 4 °C.

Analytical and spectroscopic data for **2**: Anal. Calcd for  $\text{C}_{37}\text{H}_{24}\text{NO}_{10}\text{Os}_3\text{P}$ : C, 35.72; H, 1.94; N, 1.13. Found: C, 36.11; H, 1.99; N, 1.16%. IR ( $\nu_{\text{CO}}$ ,  $\text{CH}_2\text{Cl}_2$ ): 2088s, 2047vs, 2007vs, 1992s, 1973m, 1923w  $\text{cm}^{-1}$ .  $^1\text{H}$  NMR ( $\text{CDCl}_3$ , 25 °C):  $\delta$  9.20 (dd, J 5.2, 1.6 Hz, 1H), 7.88 (dd, J 8.0, 1.6 Hz, 1H), 7.38 (d, J 2.4 Hz, 1H), 7.30 (m, 4H), 7.20 (m, 11H), 6.97 (dd, J 5.2, 8.0 Hz, 1H), 6.32 (d, J 2.4 Hz, 1H), 3.58 (s, 3H), -11.76 (d,  $J_{\text{PH}}$  15.6 Hz, 1H).  $^{31}\text{P}\{^1\text{H}\}$  NMR ( $\text{CDCl}_3$ , 25 °C):  $\delta$  12.6 (s, 1P).

#### 4.3. Thermolysis of $[\text{Os}_3(\text{CO})_9(\text{PPh}_3)\{\mu\text{-}\eta^1, \kappa^1\text{-C}_9\text{H}_5\text{N}(6\text{-OMe})\}(\mu\text{-H})]$ **2**

A toluene solution (30 mL) of **2** (100 mg, 0.080 mmol) was heated at 110 °C for 5 h. After removal of the solvent under reduced pressure, the residue was subjected to TLC on silica gel. Elution with hexane/ $\text{CH}_2\text{Cl}_2$  (1:1, v/v) developed seven bands, which afforded the following compounds in order of elution:  $[\text{Os}_3(\text{CO})_9(\text{PPh}_3)\{\mu\text{-}\eta^1, \kappa^1\text{-C}_9\text{H}_5\text{N}(6\text{-OMe})\}(\mu\text{-H})]$  (**3**) (16 mg, 15%),  $[\text{Os}_3(\text{CO})_9(\text{PPh}_3)\{\mu\text{-}\eta^1, \kappa^1\text{-C}_9\text{H}_5\text{N}(6\text{-OMe})\}(\mu\text{-H})]$  (**4**) (18 mg, 18%), **1** (2 mg, 3%), **2** (2 mg, 2%) as yellow crystals,  $[\text{Os}_3(\text{CO})_8(\text{PPh}_3)\{\mu_3\text{-}\eta^1, \kappa^1\text{-C}_9\text{H}_5\text{N}(6\text{-OMe})\}(\mu\text{-H})]$

H)] (**5**) (5 mg, 5%),  $[\text{Os}_3(\text{CO})_7\{\mu\text{-}\eta^1, \kappa^1\text{-PPh}_2(\text{C}_6\text{H}_4)\}\{\mu_3\text{-}\eta^1, \kappa^1\text{-C}_9\text{H}_5\text{N}(\text{OMe})\}(\mu\text{-H})_2]$  (**6**) (19 mg, 20%) as red crystals and  $[\text{Os}_3(\text{CO})_6(\text{PPh}_3)\{\mu\text{-}\eta^1, \kappa^1\text{-PPh}_2(\text{C}_6\text{H}_4)\}\{\mu_3\text{-}\eta^1, \kappa^1\text{-C}_9\text{H}_5\text{N}(\text{OMe})\}(\mu\text{-H})_2]$  (**7**) (18 mg, 16%) as green crystals after recrystallization from hexane/ $\text{CH}_2\text{Cl}_2$  at 4 °C.

Analytical and spectroscopic data for **3**: Anal. Calcd for  $\text{C}_{37}\text{H}_{25}\text{Cl}_2\text{NO}_{10}\text{Os}_3\text{P}\cdot\text{CH}_2\text{Cl}_2$ : C, 34.36; H, 1.90; N, 1.05. Found: C, 34.92; H, 1.99; N, 1.09%. IR ( $\nu\text{CO}$ ,  $\text{CH}_2\text{Cl}_2$ ): 2084s, 2041vs, 2009vs, 1991s, 1978w, 1958w  $\text{cm}^{-1}$ .  $^1\text{H}$  NMR ( $\text{CDCl}_3$ , 25 °C):  $\delta$  8.51 (dd, J 1.6, 5.2 Hz, 1H), 8.13 (d, J 2.8 Hz, 1H), 7.61 (d, J 8.0 Hz, 1H), 7.36 (m, 4H), 7.21 (m, 11H), 6.52 (d, J 3.2 Hz, 1H), 6.31 (dd, J 5.2, 8.0 Hz, 1H), 3.88 (s, 3H), -12.13 (d,  $J_{\text{PH}}$  16.8 Hz, 1H).  $^{31}\text{P}\{^1\text{H}\}$  NMR ( $\text{CDCl}_3$ , 25 °C):  $\delta$  13.9 (s).

Analytical and spectroscopic data for **4**: Anal. Calcd for  $\text{C}_{37}\text{H}_{24}\text{NO}_{10}\text{Os}_3\text{P}$ : C, 35.72; H, 1.94; N, 1.13. Found: C, 35.06; H, 1.97; N, 1.17%. IR ( $\nu\text{CO}$ ,  $\text{CH}_2\text{Cl}_2$ ): 2083m, 2049vs, 2018vs, 1999vs, 1971m, 1955m, 1943w  $\text{cm}^{-1}$ .  $^1\text{H}$  NMR ( $\text{CDCl}_3$ , 25 °C):  $\delta$  9.57 (dd, J 1.2, 5.6 Hz, 1H), 8.31 (d, J 2.8 Hz, 1H), 7.89 (dd, J 1.2, 8.0 Hz, 1H), 7.35 (m, 15H), 7.06 (dd, J 5.6, 8.0 Hz, 1H), 6.63 (d, J 2.8 Hz, 1H), 3.96 (s, 3H), -15.58 (d,  $J_{\text{PH}}$  14.0 Hz, 1H).  $^{31}\text{P}\{^1\text{H}\}$  NMR ( $\text{CDCl}_3$ , 25 °C):  $\delta$  -3.2 (s).

Analytical and spectroscopic data for **5**: Anal. Calcd for  $\text{C}_{36}\text{H}_{24}\text{NO}_9\text{Os}_3\text{P}$ : C, 35.55; H, 1.99; N, 1.15. Found: C, 35.88; H, 2.05; N, 1.21%. IR ( $\nu\text{CO}$ ,  $\text{CH}_2\text{Cl}_2$ ): 2058s, 2020vs, 1989m, 1977s, 1949m, 1930w  $\text{cm}^{-1}$ .  $^1\text{H}$  NMR ( $\text{CD}_2\text{Cl}_2$ , 25 °C):  $\delta$  9.48 (dd, J 1.6, 5.2 Hz, 1H), 8.35 (d, J 2.8 Hz, 1H), 7.91 (dd, J 1.6, 7.6 Hz, 1H), 7.38 (m, 15H), 7.12 (dd, J 5.2, 7.6 Hz, 1H), 6.58 (d, J 2.8 Hz, 1H), 3.94 (s, 3H), -10.25 (d,  $J_{\text{PH}}$  7.6 Hz, 1H).  $^{31}\text{P}\{^1\text{H}\}$  NMR ( $\text{CD}_2\text{Cl}_2$ , 25 °C):  $\delta$  22.2.

Analytical and spectroscopic data for **6**: Anal. Calcd for  $\text{C}_{35}\text{H}_{24}\text{NO}_8\text{Os}_3\text{P}$ : C, 35.38; H, 2.04; N, 1.18. Found: C, 35.75; H, 2.12; N, 1.23%. IR ( $\nu\text{CO}$ ,  $\text{CH}_2\text{Cl}_2$ ): 2063vs, 2016s, 1996vs, 1982s, 1949m  $\text{cm}^{-1}$ .  $^1\text{H}$  NMR ( $\text{CD}_2\text{Cl}_2$ , 25 °C):  $\delta$  9.22 (d, J 3.6 Hz, 1H), 8.37 (d, J 3.6 Hz, 1H), 8.13 (m, 1H), 8.04 (d, J 8.4 Hz, 1H), 7.57 (m, 1H), 7.36 (m, 10H), 7.11 (m, 4H) 3.39 (s, 3H), -9.04 (d,  $J_{\text{PH}}$  12.4 Hz, 1H), -11.43 (s, 1H).  $^{31}\text{P}\{^1\text{H}\}$  NMR ( $\text{CDCl}_3$ , 25 °C):  $\delta$  -22.9 (s).

Analytical and spectroscopic data **7**: Anal. Calcd for  $\text{C}_{52}\text{H}_{39}\text{NO}_7\text{Os}_3\text{P}_2$ : C, 43.91; H, 2.76; N, 0.98. Found: C, 44.38; H, 2.83; N, 1.03%. IR ( $\nu\text{CO}$ ,  $\text{CH}_2\text{Cl}_2$ ): 2018m, 2000vs, 1972w, 1945s  $\text{cm}^{-1}$ .  $^1\text{H}$  NMR ( $\text{CDCl}_3$ , 25 °C):  $\delta$  8.29 (d, J 2.4 Hz, 1H), 8.14 (m, 2H), 7.69 (d, J 7.6 Hz, 1H), 7.50 (m, 4H), 7.36 (m, 21H), 7.11 (m, 4H), 6.27 (dd, J 7.6, 5.2 Hz, 1H), 3.34 (s, 3H), -8.76 (dd, J 12.0, 2.4 Hz, 1H), -11.22 (d, J 18.0 Hz, 1H).  $^{31}\text{P}\{^1\text{H}\}$  NMR ( $\text{CDCl}_3$ , 25 °C):  $\delta$  13.2 (s, 1P), -18.2 (s, 1P).

#### 4.4. Thermolysis of **3**

By a procedure similar to that described above, thermolysis of **3** (50 mg, 0.038 mmol) at 110 °C for 5 h followed by similar chromatographic separation gave the following compounds in order of elution: **3** (1 mg, 2%), **4** (10 mg, 21%), **5** (3 mg, 7%), **6** (9 mg, 20%) and **7** (6 mg, 11%).

#### 4.5. Thermolysis of **4**

A toluene solution (20 mL) of **4** (25 mg, 0.020 mmol) was heated to reflux for 5 h. A similar chromatographic work up described above afforded **5** (2 mg, 8%), **6** (7 mg, 29%) and **7** (5 mg, 17%).

#### 4.6. Thermolysis of **5**

A toluene solution (20 mL) of **5** (25 mg, 0.021 mmol) was heated to reflux for 5 h. A similar chromatographic work up described above afforded unreacted **5** (3 mg), **6** (9 mg, 37%) and **7** (6 mg, 21%).

#### 4.7. Reaction of **6** with $PPh_3$

A toluene solution (20 mL) of **6** (25 mg, 0.021 mmol) and  $PPh_3$  (7 mg, 0.046 mmol) was heated to reflux at 110 °C for 4 h. A similar chromatographic separation described above developed two bands which afforded unreacted **6** (5 mg) and **7** (10 mg, 33%) in order of elution.

#### 4.8. Crystal structure determination

Single crystals of **2**, **3**, **6** and **7** suitable for single-crystal X-ray diffraction analyses were grown by slow diffusion of hexane into a  $CH_2Cl_2$  solution. Suitable crystals of **2** and **3** were mounted on an Agilent Super Nova dual diffractometer (Agilent Technologies Inc., Santa Clara, CA) using a Nylon loop with inert oil and the diffraction data were collected at 150(1) K using Mo- $K\alpha$  radiation ( $\lambda = 0.71073$ ). Unit cell determination, data reduction, and absorption corrections were carried out using CrysAlisPro [28]. The structures were solved

with the Sir2004 [29] structure solution program by direct methods or Charge Flipping [30] and refined by full-matrix least-squares on the basis of  $F^2$  using SHELX 2013 [31] within the OLEX2 [32] graphical user interface. Non-hydrogen atoms were refined anisotropically, and hydrogen atoms (except those directly bonded to metals) were included using a riding model.

Suitable single crystals of **6** and **7** were mounted on a Bruker SMART APEX CCD diffractometer using glass fiber and the diffraction data were collected at 173(2) K (**6**) or 172(2) K (for **7**) using Mo-K $\alpha$  radiation ( $\lambda = 0.71073$ ). Data reduction and integration were carried out with SAINT+ and absorption corrections were applied using the program SADABS [33]. Structures were solved by direct methods and refined using full-matrix least-squares on  $F^2$ . All non-hydrogen atoms were refined anisotropically. Hydrogen atoms were included in a riding model. The hydride was positioned by using the XHYDEX program in the WinGX suite of programs [34]. The SHELXTL PLUS V6.10 program package was used for structure solution and refinement [35]. Pertinent crystallographic parameters are given in Table 1.

## 5. Acknowledgements

This research has been sponsored by the Ministry of Science and Technology, Government of the People's Republic of Bangladesh.

## 6. Supplementary data

CCDC 1820920, CCDC 1820921, CCDC 1820922 and CCDC 1820923 contain supplementary crystallographic data for **2**, **3**, **6** and **7**, respectively. These data may be obtained free of charge from The Cambridge Crystallographic Data Center via [www.ccdc.cam.ac.uk/data\\_request/cif](http://www.ccdc.cam.ac.uk/data_request/cif).

**Table 1. Crystallographic data and structure refinement details for 2, 3, 6 and 7**

Compound	2	3	6	7
CCDC registry number	1820920	1820921	1820922	1820923
Empirical formula	C <sub>37</sub> H <sub>24</sub> NO <sub>10</sub> Os <sub>3</sub> P	C <sub>38</sub> H <sub>25</sub> Cl <sub>2</sub> NO <sub>10</sub> Os <sub>3</sub> P	C <sub>35</sub> H <sub>24</sub> NO <sub>8</sub> Os <sub>3</sub> P	C <sub>52</sub> H <sub>39</sub> NO <sub>7</sub> Os <sub>3</sub> P
Formula weight	1244.14	1328.06	1188.12	1422.38
Temperature (K)	150(1)	150(1)	173(2)	172(2)
Wavelength (Å)	0.71073	0.71073	0.71073	0.71073
Crystal system	Monoclinic	Monoclinic	Monoclinic	Triclinic
Space group	P2 <sub>1</sub> /n	P2 <sub>1</sub> /n	P2 <sub>1</sub> /n	P-1
a (Å)	9.8027(2)	12.29530(14)	10.0640(10)	11.491(2)
b (Å)	32.7034(7)	19.1781(2)	17.7576(18)	14227(3)
c (Å)	11.3073(2)	16.6071(2)	19.1119(19)	14813(3)
α (°)	90	90	90	86.608(4)
β (°)	104.019(2)	95.1752(11)	103.510(2)	85.060(4)
γ (°)	90	90	90	87.097(3)
Volume (Å <sup>3</sup> )	3516.93(13)	3900.01(8)	3321.0(6)	2405.7(8)
Z	4	4	4	2
Calculated density (g/m <sup>3</sup> )	2.350	2.262	2.376	1.964
Absorption coefficient (mm <sup>-1</sup> )	10.918	9.986	11.552	8.022
F(000)	2304.0	2468.0	2192	1344
Crystal size (mm)	0.22 × 0.08 × 0.02	0.28 × 0.11 × 0.10	0.52 × 0.32 × 0.22	0.36 × 0.18 × 0.09
2θ range for data collection (°)	5.356 to 56.92	5.806 to 56.95	3.18 to 56.64	2.88 to 56.54
Reflections collected	56781	66814	34189	19634
Independent reflections ( <i>R</i> <sub>int</sub> )	6859 [0.0379]	7630 [0.0543]	8259 [0.0447]	10133 [0.0230]
Completeness to theta	26.00, 99.5%	26.00, 99.5%	28.28, 99.7%	26.99, 96.4.0%
Max. and min. transmission	1.000 and 0.352	1.000 and 0.478	0.185 and 0.065	0.532 and 0.160
Data / restraints / parameters	6859/0/474	7630/0/505	8259/0/434	10133/0/595
Goodness-of-fit on <i>F</i> <sup>2</sup>	1.176	1.071	1.088	0.995
Final R indices [ <i>I</i> > 2σ( <i>I</i> )]	R <sub>1</sub> = 0.0232, wR <sub>2</sub> = 0.0406	R <sub>1</sub> = 0.0214, wR <sub>2</sub> = 0.0487	R <sub>1</sub> = 0.0273, wR <sub>2</sub> = 0.0637	R <sub>1</sub> = 0.0285, wR <sub>2</sub> = 0.0693
Largest diff. peak/ hole (e.Å <sup>-3</sup> )	1.19 and -1.95	2.68 and -1.84	1.333 and -0.966	1.66 and -1.26

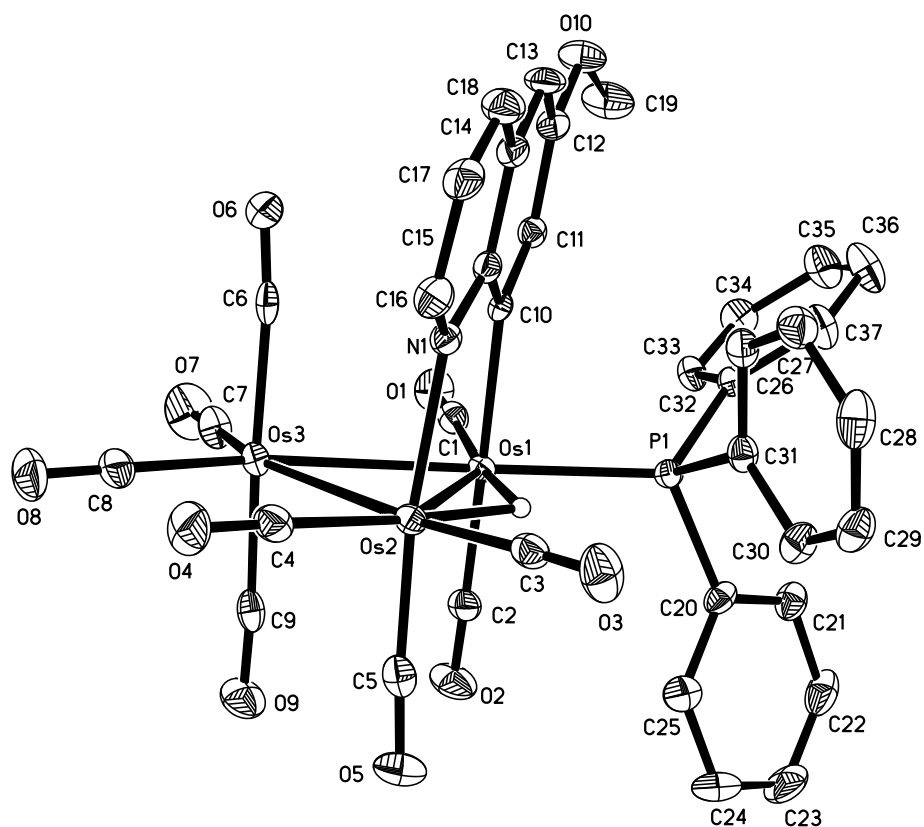


**Fig. 1.** An ORTEP diagram of the solid-state molecular structure of  $[\text{Os}_3(\text{CO})_9(\text{PPh}_3)\{\mu\text{-}\eta^1, \kappa^1\text{-C}_9\text{H}_5\text{N}(6\text{-OMe})\}(\mu\text{-H})]$  (**2**) showing 50% probability thermal ellipsoids. Hydrogen atoms except the bridging hydrides are omitted for clarity. Selected bond lengths ( $\text{\AA}$ ) and angles ( $^\circ$ ): Os(1)–Os(2) 2.9009(2), Os(1)–Os(3) 2.9046(2), Os(2)–Os(3) 2.8928(2), Os(2)–N(1) 2.170(3), Os(1)–C(10) 2.157(4), Os(1)–P(1) 2.3687(11), Os(2)–Os(1)–Os(3) 59.774(6), Os(1)–Os(2)–Os(3) 60.178(6), Os(1)–Os(3)–Os(2) 60.049(5), P(1)–Os(1)–Os(2) 107.41(3), P(1)–Os(1)–Os(3) 166.59(3), P(1)–Os(1)–C(10) 85.74(11), Os(1)–Os(2)–N(1) 84.54(9), Os(3)–Os(2)–N(1) 90.51(9), Os(2)–Os(1)–C(10) 83.50(11), Os(3)–Os(1)–C(10) 88.66(10).

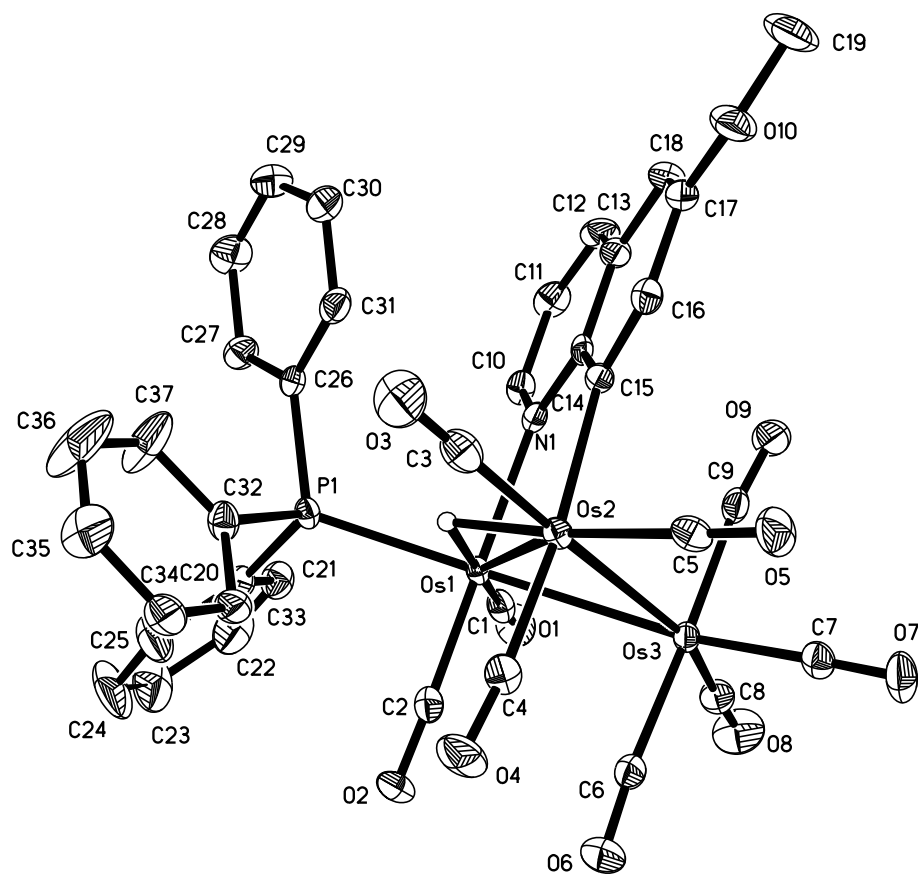


**Fig. 2.** An ORTEP diagram of the solid-state molecular unit of  $[\text{Os}_3(\text{CO})_9(\text{PPh}_3)\{\mu\text{-}\eta^1, \kappa^1\text{-C}_9\text{H}_5\text{N}(6\text{-OMe})\}(\mu\text{-H})]$  (**3**) showing 50% probability thermal ellipsoids. Hydrogen atoms except the bridging hydrides are omitted for clarity. Selected bond lengths (Å) and angles (°): Os(1)–Os(2) 2.8965(2), Os(1)–Os(3) 2.8936(2), Os(2)–Os(3) 2.9131(2), Os(1)–N(1) 2.189(3), Os(1)–P(1) 2.3690(10), Os(2)–C(15) 2.155(4), Os(2)–Os(1)–Os(3) 60.412(5), Os(1)–Os(2)–Os(3) 59.745(5), Os(1)–Os(3)–Os(2) 59.843(5), P(1)–Os(1)–Os(2) 109.60(2), P(1)–Os(1)–Os(3) 169.82(2), P(1)–Os(1)–N(1) 91.01(8), Os(2)–Os(1)–N(1) 84.26(8), Os(3)–Os(1)–N(1) 89.89(8), Os(1)–N(1)–C(14) 125.1(2), Os(1)–Os(2)–C(15) 83.81(10), Os(3)–Os(2)–C(15) 90.77(10).

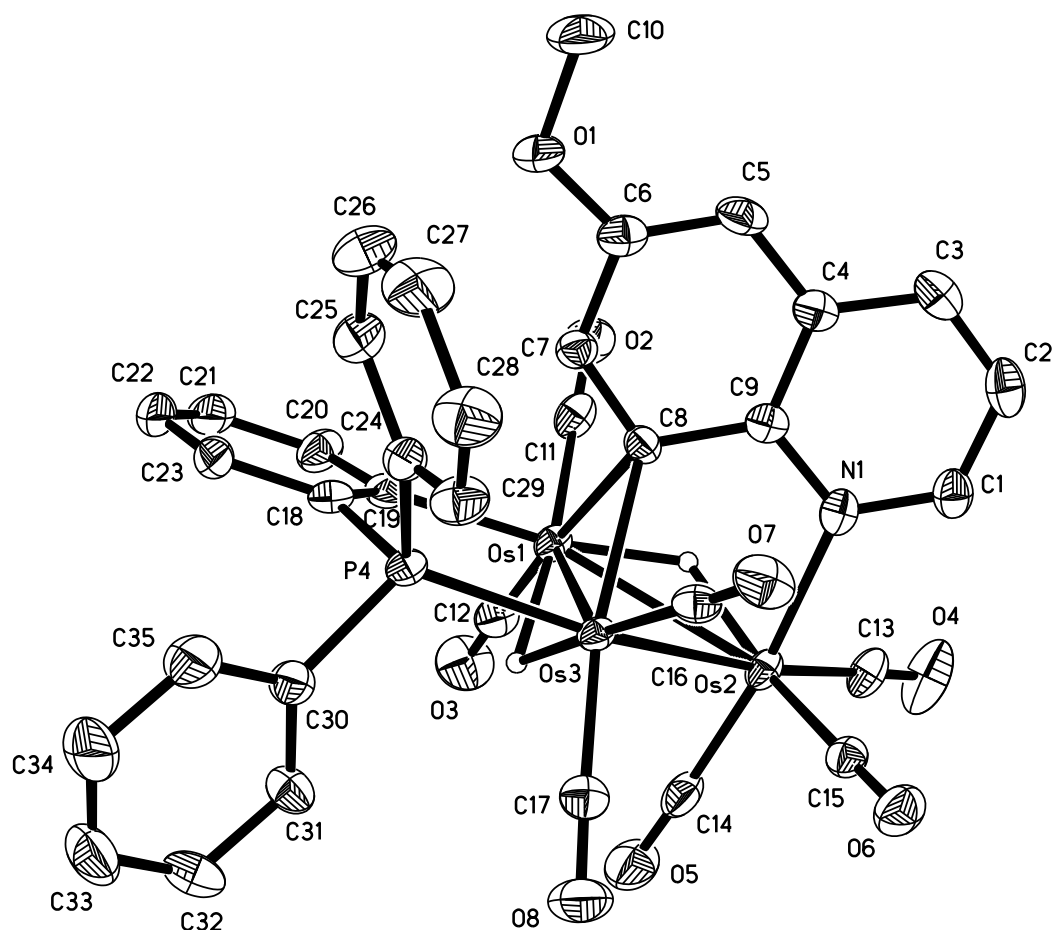


**Fig. 3.** An ORTEP diagram of the solid-state molecular structure of  $[\text{Os}_3(\text{CO})_7\{\mu\text{-}\eta^1, \kappa^1\text{-PPh}_2(\text{C}_6\text{H}_4)\}\{\mu_3\text{-}\eta^1, \kappa^1\text{-C}_9\text{H}_5\text{N}(\text{OMe})\}(\mu\text{-H})_2]$  (**6**) showing 50% probability thermal ellipsoids. Hydrogen atoms except the bridging hydrides are omitted for clarity. Selected bond lengths (Å) and angles (°): Os(1)–Os(2) 2.9548(3), Os(1)–Os(3) 2.7043(3), Os(2)–Os(3) 2.7733(3), Os(2)–N(1) 2.151(4), Os(3)–P(4) 2.3473(11), Os(1)–C(19) 2.128(5), Os(1)–C(8) 2.316(4), Os(3)–C(8) 2.329(4), Os(1)–Os(2)–Os(3) 56.236(6), Os(1)–Os(3)–Os(2) 65.276(8), Os(3)–Os(1)–Os(2) 58.488(9), P(4)–Os(3)–Os(2) 155.64(3), P(4)–Os(3)–Os(1) 90.47(3), Os(1)–Os(2)–N(1) 87.34(10), Os(3)–Os(2)–N(1) 84.39(10).

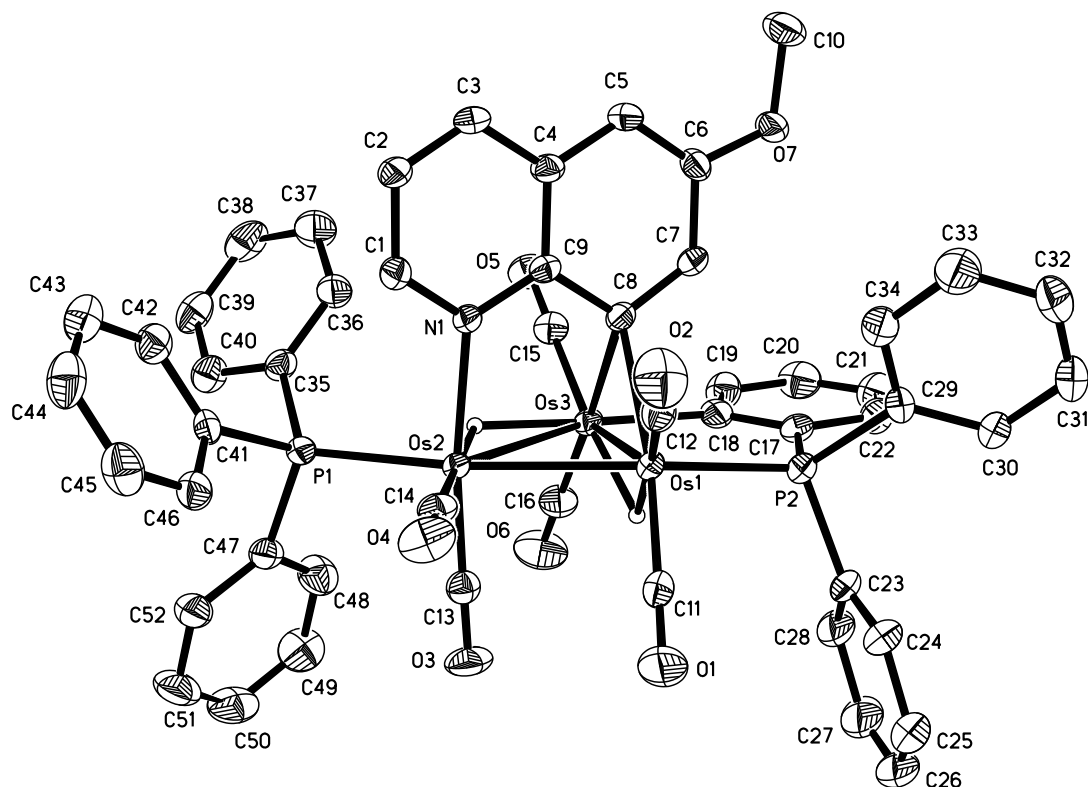


**Fig. 4.** An ORTEP diagram of the solid-state molecular structure of  $[\text{Os}_3(\text{CO})_6(\text{PPh}_3)\{\mu\text{-}\eta^1, \kappa^1\text{-PPh}_2(\text{C}_6\text{H}_4)\}\{\mu_3\text{-}\eta^1, \kappa^1\text{-C}_9\text{H}_5\text{N}(\text{OMe})\}(\mu\text{-H})_2]$  (**7**) showing 50% probability thermal ellipsoids. Hydrogen atoms except the bridging hydrides are omitted for clarity. Selected bond lengths ( $\text{\AA}$ ) and angles ( $^\circ$ ): Os(1)–Os(2) 2.7765(5), Os(1)–Os(3) 2.7152(5), Os(2)–Os(3) 2.9918(5), Os(2)–N(1) 2.167(3), Os(2)–P(1) 2.3903(12), Os(1)–P(2) 2.3581(13), Os(3)–C(18) 2.138(5), Os(1)–C(8) 2.329(4), Os(3)–C(8) 2.334(4), Os(1)–Os(2)–Os(3) 56.011(9), Os(1)–Os(3)–Os(2) 57.981(14), Os(3)–Os(1)–Os(2) 66.009(10), P(1)–Os(2)–Os(3) 112.20(3), P(2)–Os(1)–Os(2) 154.47(4), Os(1)–Os(2)–N(1) 83.66(10), Os(3)–Os(2)–N(1) 86.74(10), P(1)–Os(2)–Os(1) 168.01(3).

## References

- [1] E. Rosenberg, R. Kumar, *Dalton Trans.* 41 (2012) 714.
- [2] M.J. Abedin, B. Bergman, R. Holmquist, R. Smith, E. Rosenberg, J. Ciurash, K. Hardcastle, J. Roe, V. Vazquez, C. Roe, S. Kabir, B. Roy, S. Alam, K.A. Azam, *Coord. Chem. Rev.* 190–192 (1999) 975.
- [3] S.E. Kabir, D.S. Kolwaite, E. Rosenberg, K. Hardcastle, W. Cresswell, J. Grindstaff, *Organometallics* 14 (1995) 3611.
- [4] S.E. Kabir, D.S. Kolwaite, E. Rosenberg, L.G. Scott, T. McPhillips, R. Duque, M. Day, K.I. Hardcastle, *Organometallics* 15 (1996) 1979.
- [5] E. Arcia, D.S. Kolwaite, E. Rosenberg, K. Hardcastle, J. Ciurash, R. Duque, R. Gobetto, L. Milone, D. Osella, M. Botta, W. Dastrú, A. Viale, I. Fiedler, *Organometallics*, 17 (1998) 415.
- [6] A.B. Din, B. Bergman, E. Rosenberg, R. Smith, W. Dastru, R. Gobetto, L. Milone, A. Viale, *Polyhedron* 17 (1998) 2975.
- [7] B. Bergman, R. Holmquist, R. Smith, E. Rosenberg, J. Ciurash, K. Hardcastle, M. Visi, *J. Am. Chem. Soc.* 120 (1998) 12818.
- [8] R. Smith, E. Rosenberg, K.I. Hardcastle, V. Vazquez, J. Roh, *Organometallics* 18 (1999) 3519.
- [9] E. Rosenberg, M.J. Abedin, D. Rokhsana, D. Osella, L. Milone, C. Nervi, J. Fiedler, *Inorg. Chim. Acta* 300–302 (2000) 769.
- [10] S.E. Kabir, K.M.A. Malik, H.S.Mandal, M.A. Mottalib, M.J. Abedin, E. Rosenberg, *Organometallics* 21 (2002) 2593.
- [11] E. Rosenberg, M.J. Abedin, D. Rokhsana, A. Viale, W. Dastru, R. Gobetto, L. Milone, K. Hardcastle, *Inorg. Chim. Acta* 334 (2002) 343.
- [12] C. Nervi, R. Gobetto, L. Milone, A. Viale, E. Rosenberg, D. Rokhsana, J. Fiedler, *Chem. Eur. J.* 9 (2003) 5749.
- [13] E. Rosenberg, F. Spada, K. Sugden, B. Martin, L. Milone, R. Gobetto, A. Viale, J. Fiedler, *J. Organomet. Chem.* 668 (2003) 51.
- [14] E. Rosenberg, D. Rokhsana, C. Nervi, R. Gobetto, L. Milone, A. Viale, J. Fiedler, M.A. Botavina, *Organometallics* 23 (2004) 215.
- [15] E. Rosenberg, S.E. Kabir, M.J. Abedin, K.I. Hardcastle, *Organometallics* 23 (2004) 3982.

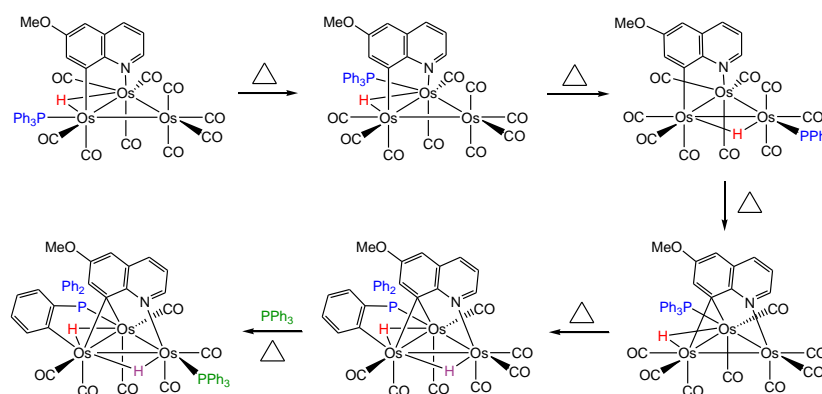
- [16] E. Rosenberg, F. Spada, K. Sugden, B. Martin, R. Gobetto, L. Milone, A. Viale, J. Organomet. Chem. 689 (2004) 4729.
- [17] M.A. Mottalib, N. Begum, S.M.T. Abedin, T. Akter, S.E. Kabir, M.A. Miah, D. Rokhsana, E. Rosenberg, G.M.G. Hossain, K.I. Hardcastle, Organometallics 24 (2005) 4747.
- [18] D.G. Musaev, T. Nowroozi-Isfahani, K. Morokuma, E. Rosenberg, Organometallics 24 (2005) 5973.
- [19] D. Colangelo, A.L. Ghiglia, A.R. Ghezzi, M. Ravera, E. Rosenberg, F. Spada, D. Osella, J. Inorg. Biochem. 99 (2005) 505.
- [20] D.G. Musaev, T. Nowroozi-Isfahani, K. Morokuma, J. Abedin, E. Rosenberg, K. I. Hardcastle, Organometallics 25 (2006) 203.
- [21] T. Nowroozi-Isfahani, D.G. Musaev, K. Morokuma, E. Rosenberg, Inorg. Chem. 45 (2006) 4963.
- [22] A.K. Raha, S. Ghosh, M.M. Karim, D.A. Tocher, N. Begum, A. Sharmin, E. Rosenberg, S.E. Kabir, J. Organomet. Chem. 693 (2008) 3613.
- [23] S. Ghosh, M.N. Uddin, N. Begum, G.M.G. Hossain, K.A. Azam, S.E. Kabir, J. Chem. Crystallogr. 40 (2010) 572.
- [24] M.I. Hossain, S. Ghosh, G. Hogarth, G.M.G. Hossain, S.E. Kabir, J. Organomet. Chem. 696 (2011) 3036.
- [25] S. Ghosh, M.R. Al-Mamun, G.M.G. Hossain, S.E. Kabir, Inorg. Chim. Acta 378 (2011) 307.
- [26] E. Rosenberg, J. Abedin, K. I. Hardcastle, J. Clust. Sci. 23 (2012) 901.
- [27] S.A. Begum, Md.A.H. Chowdhury, S. Ghosh, D.A. Tocher, M.G. Richmond, E. Rosenberg, S.E. Kabir, J. Organomet. Chem. 849-850 (2017) 337.
- [28] CrysAlisPro; Oxford Diffraction: Yarnton, England, 2015.
- [29] R. Caliendo, B. Carrozzini, G.L. Cascarano, C. Giacovazzo, A. Mazzone, D.J. Siliqi, Appl. Crystallogr. 42 (2009) 302-307.
- [30] L. Palatinus, G. Chapuis, J. Appl. Crystallogr. 40 (2007) 786-790.
- [31] G.M. Sheldrick, Acta Crystallogr., Sect. A: Found. Crystallogr. 64 (2008) 112-122.
- [32] O.V. Dolomanov, L.J. Bourhis, R.J. Gildea, J.a.K. Howard, H. Puschmann, J. Appl. Crystallogr. 42 (2009) 339-341.
- [33] SMART and SAINT software for CCD diffractometers, version 6.1, Madison, WI (2000).
- [34] L.J. Farrugia, J. Appl. Crystallogr. 32 (1999) 837.

## Graphical Abstract

### Reaction of electron-deficient 6-methoxyquinolinate-substituted cluster $[\text{Os}_3(\text{CO})_9\{\mu_3\text{-}\eta^1, \kappa^1\text{-C}_9\text{H}_5\text{N}(6\text{-OMe})\}(\mu\text{-H})]$ with $\text{PPh}_3$ : Thermally induced ligand isomerization, decarbonylation and orthometallation

Shahin A. Begum, Md. Arshad H. Chowdhury, Shishir Ghosh, Derek A. Tocher, Edward Rosenberg, Kenneth I. Hardcastle, Shariff E. Kabir

The reactivity of electron-deficient triosmium cluster  $[\text{Os}_3(\text{CO})_9\{\mu_3\text{-}\eta^1, \kappa^1\text{-C}_9\text{H}_5\text{N}(6\text{-OMe})\}(\mu\text{-H})]$  towards  $\text{PPh}_3$  has been investigated.



## Research Highlights

- $\text{PPh}_3$  substitution reactivity at 6-methoxyquinolinate-substituted  $\text{Os}_3$  clusters
- Hydride/phosphine isomerization in  $[\text{Os}_3(\text{CO})_9(\text{PPh}_3)\{\mu\text{-}\eta^1, \kappa^1\text{-C}_9\text{H}_5\text{N}(6\text{-OMe})\}(\mu\text{-H})]$  clusters
- $\text{Os}_3$  clusters with edge-bridged and face-capped 6-methoxyquinolinate ligands